



Paper Type: Original Article

## Designing and Developing a 3D Model of Solar Array Deployment Mechanism for a 1U Cubesat

Iyenagbe Benjamin Ugheoke<sup>1,\*</sup> , Nasir Muhammed Lawal<sup>1</sup>

<sup>1</sup> Department of Mechanical Engineering, University of Abuja, Nigeria. ben.ugheoke@uniabuja.edu.ng, nasir.lawal@uniabuja.edu.ng.

### Citation:

Received: 08 July 2024  
Revised: 02 August 2024  
Accepted: 18 August 2024

Ugheoke, I. B., & Lawal, N. M. (2024). Designing and developing a 3D model of solar array deployment mechanism for a 1U cubesat. *Intelligence modeling in electromechanical systems*, 1 (1), 39-54.


### Abstract

Satellites are part of many innovations and inventions that significantly impact the global economy, particularly in precision agriculture, security, water management, disaster control and management, and environmental and weather monitoring. However, it is expensive for developing countries to acquire large space infrastructure such as satellites easily, hence using smaller crafts like the CubeSats. One cheap way to acquire CubeSats is by creating complex parts through reverse engineering. This would help keep the high capital expenditure rate in check and turn such countries from consumer nations to nations that produce their goods. This article discusses the design, synthesis, modelling, and component sizing of a solar panel array deployment mechanism for 1-U CubeSat to improve dynamic performance, weight optimization, system stability, and photovoltaic surface projection for maximum power generation. The design has a geometric dimension of 10.5 cm x 10.3 cm x 10.7 cm (in launch configuration) with two opposite wings. Each wing has two-panel mounts, having a length of 70 mm per panel, an inter-panel hinge space of 5.41 mm to allow for free rotation, and a yoke length of 35.64 mm, given a combined wing space length of 181.05 mm. With a limiting width of about 10 cm, the maximum combined (end-to-end) length for two foldable mounts (arms) was chosen not to exceed 20 cm on each side of the CubeSat. Dynamic tests revealed that an overall spring stiffness of 0.0263 Nm/rad is required to move the solar panels with a resultant torque of 0.0413 Nm from 0° to 90°. The complete panel deployment was achieved in 0.078 secs with an angular velocity of 20.2084 rad/sec, but it was relaxed to 2 secs to avoid bounds back oscillation due to reverse momentum.


**Keywords:** CubeSat, Deployable solar array, Design synthesis, Component sizing, 3D printing.

## 1 | Introduction

Space technology is a strategic tool for socio-economic development as it paves the way for many programs and projects vital to a society's industrial growth and development, which benefit the people. Thus, the role of satellites, especially earth observation satellites, in the global economy cannot be over-emphasized,

 Corresponding Author: ben.ugheoke@uniabuja.edu.ng



 Licensee System Analytics. This article is an open access article distributed under the terms and conditions of the Creative Commons Attribution (CC BY) license (<http://creativecommons.org/licenses/by/4.0>).

particularly in precision agriculture, security, water management, environmental and weather monitoring, and disaster management, among others.

Recently, space technologies have focused more on designing and developing components or devices that are lighter, smaller, and cheaper, yet even more functional in the mission they were designed for. The great feats in space exploration would not have been possible because of the enormous costs involved, but they would have been possible for the entrance of miniaturized electronic circuits. These mini circuits brought about the innovation of feasibly sized computers that helped to manage, coordinate, and run the various processes within the host spacecraft. Hence, with the miniaturization of onboard components, satellites are now designed in Micro, Nano, and Pico sizes, with components as functional and effective as the big satellites.

CubeSat is a Nano satellite with an average mass of about 1.3 kg. The smallest satellite is the Pico satellite, with a mass range of 0.1 kg to 1 kg. The advantages of Nano and Pico satellites over bigger satellites include low cost and lesser handling; they are easier to launch singularly or in multiples due to their lesser weight, and quicker to access space due to their small nature, thus allowing non-space faring nations and corporations to have access to the space. Technically, CubeSats are self-dependent, fast to set up, and versatile for applications. They have been used for research, low earth orbit applications like remote sensing, earth science, disaster response, climate monitoring, and, recently, interplanetary missions.

However, it is expensive for developing countries to easily acquire space infrastructure like the CubeSat (50,000 to 200,000 dollars); thus, developing such infrastructure through reverse engineering would help curb capital flight and transform the country from a consumer nation to a production nation.

This work aims to design and develop a 3D model of a deployable two-panel solar array for a 1-U CubeSat, with the specific objectives to synthesize, design the solar array and its drive mechanisms using SOLIDWORKS software; implement the 3D printing and coupling of the designed components and structures; and the physical testing of the printed 3D prototype to validate the dynamic functionality of the designed deployment mechanism.

## 2 | Methodology

This section of this work reports the methodologies deployed for establishing the design (synthesis and modelling), fabrication (3D printing), and testing of the Solar Array Deployment Mechanism (SADM) (with its drive system) for a 1-U CubeSats. The methodology for the system development was divided into:

- I. The design synthesis of the SADM. This refers to modeling the solar array structures and their drive systems using SOLIDWORKS software with motion analysis, assembly performance, and simulation features.
- II. Sizing and stress analysis of deployment actuators- the spring, fisher wire, and hinges that constitute the functional revolute joints holding the solar panels together.
- III. 3D printing and coupling of the designed and modeled structures. PLA and resin were used as biodegradable thermoplastics, which are lighter and have outstanding thermal insulations.
- IV. Testing the assembly to validate deployment dynamics, such as wing loads, deployment time, and vibration.

### 2.1 | Design Synthesis Overview

The deployment mechanism utilized in this work comprises two main components: the Hold-Down and Release Mechanism (HDRM) and the SADM. In the hold-down condition, the panel arms are folded around the frame, as illustrated in *Fig. 1*. Upon deployment, the spring mechanism activates, causing the panels to spread out for optimal solar reception.

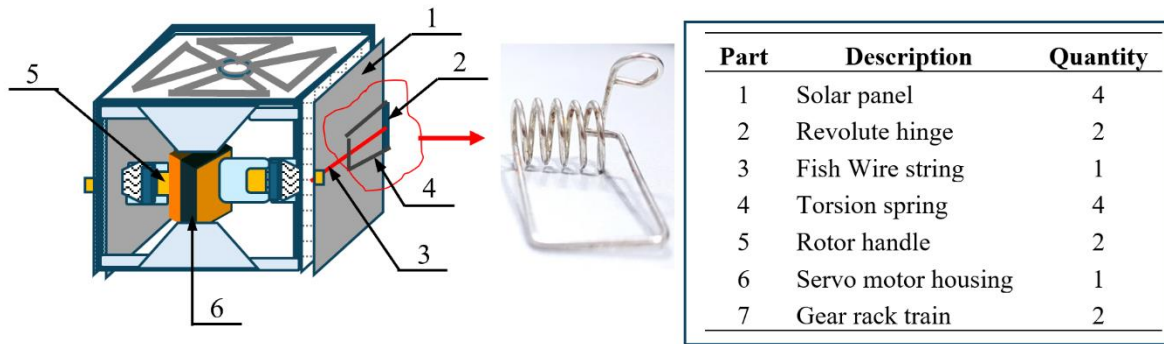


Fig. 1. Assemble CubeSat solar arms in a folded state.

Fig. 2 provides the schematic diagram of one arm of the CubeSat solar panel under deployment. Each arm of the CubeSat features two panels, labeled 1a and 1b, held in place by interlocking revolute hinges labeled 2a and 2b. A fisher wire string labeled 3 is wound on a hub, looped around the joints, and anchored to the free end of the second panel. This string functions as a damper to control speed and vibration during deployment. It keeps the panels firmly against two torsional springs, 4a and 4b, which act as deployment actuators. The arm assembly is connected to a rotor handle labeled 5, which rotates the panels to track the sun's rays using a servo motor labeled 6. The servo motor's gear meshes with a 45-degree gear rack labeled 7.

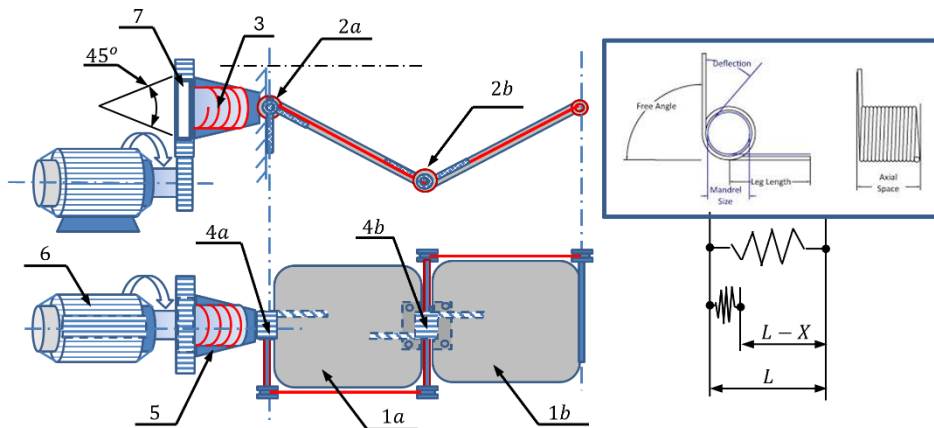


Fig. 2. Schematic diagram of the CubeSat solar panel arm with spring actuators.

## 2.2 | Working Principles

The assembled system consists of a servo motor as the primary driver to a series of connected solar array structures that are foldable and possess torsional springs at revolute joints. The array consists of two wings along the +X and -X axis, each with two arms hinged together and attached to the arm holder with a torsion spring actuator. Each arm is attached to a servo motor shaft with a bearing that rotates the yoke to 90o to the left and right towards the sun's rays. Panel 1 (and all first panels) is connected to the arm 1 torsion spring hinge, while panel 2 (and all second panels) is connected to arm 2 with another spring hinge, as shown in Fig. 3.

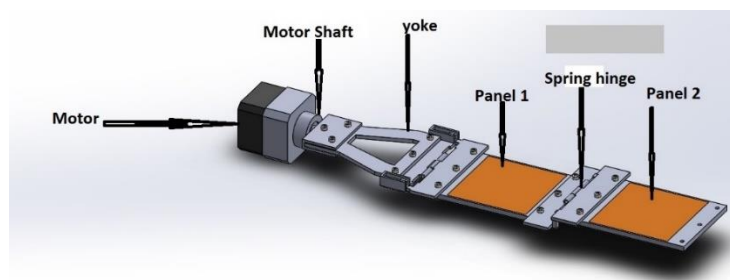


Fig. 3. Components of the solar arm.

The wings of the solar panel are stowed horizontally against the side frames of the CubeSat using an HDRM. At the prompt of the remote control or timed automated program, the hold-down pin is cut, and the tensioned spring held down by the pin gently uncoils under the control of the fisher wire to its original free state, thereby deploying each panel to an angular displacement of  $90^\circ$ .

## 2.3 | Parts Modelling

The modeled parts were generally divided into three: (i) the structural system, (ii) The deployment mechanism and operation actuators, and (iii) The drive system. Among these three, however, the electrical system is excluded from the subject of the current article for obvious reasons arising from the title of the manuscript. Thus, a suitable servo motor was selected for testing.

### 2.3.1 | The structural system

The design of the structural system includes the main body (CubeSats frame), the arms, and the PV panel sheets.

The main body is CubeSat's synthesized design, which features a structural frame measuring approximately 105 mm x 101 mm x 101 mm, with a frame thickness of 3.5 mm. This dimension aligns with the specifications commonly found in CubeSat literature [1]. *Fig. 4(a)* illustrates the modeled features of the body frame in an isometric view. To minimize weight, void spaces were strategically incorporated into the sidewalls connected by webs to maintain necessary strength. Detailed construction plans for the frame can be found in *Fig. 4(b)*.

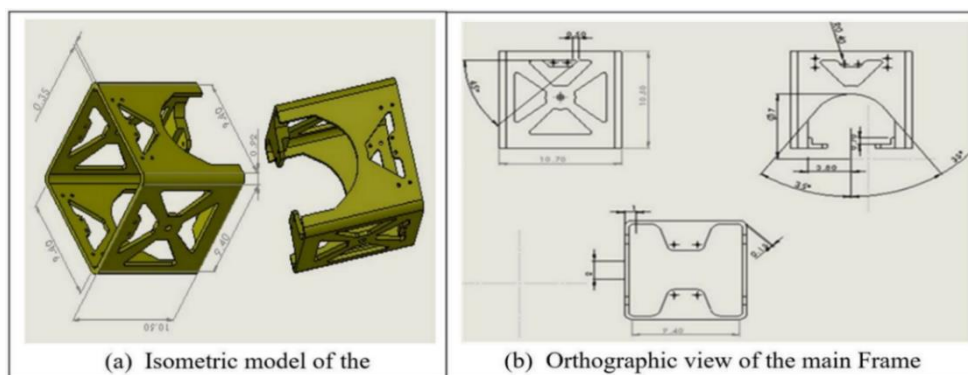


**Fig. 4. Isometric and orthographic Views of the Designed Frame of the CubeSat.**

The Solar Panel Arms provide platforms to mount the solar panels securely. They were designed with an arm-to-yoke ratio of 4, as dimensionally indicated in *Fig. 5*. Their dimensions were tailored to the CubeSat specifications. Each arm features 2 mm holes for screwing the panel sheets securely in place. A back-heel step-out base was added to prevent the second arm from moving forward, allowing it to rest on the hinge joint at the end of the first arm. This design feature halts forward motion without locking the panel in position.

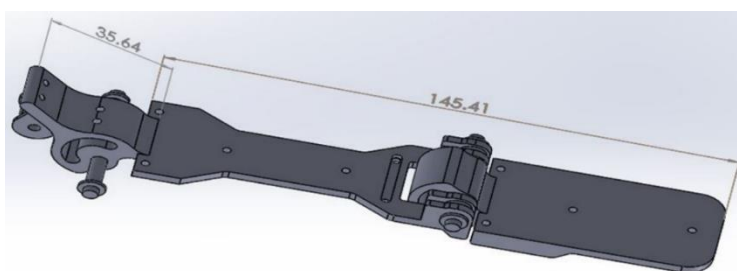


**Fig. 5. Solar array arm mount.**

A 0.5 mm thick monocrystalline solar cell with a maximum output of 2.9 W and an efficiency of 20.4% was used. The panel sheets, depicted in *Fig. 6*, are rectangular and identical, measuring 110 mm in width and 70 mm in length each and a mass density of 250 g/m<sup>2</sup>.

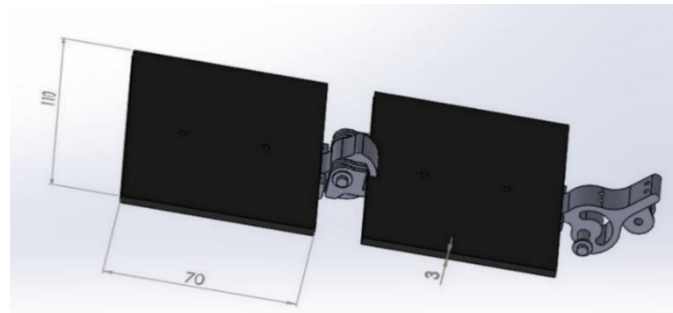


Fig. 6. Solar array panels.

### 2.3.2 | The deployment mechanism and operation actuators

The units that require design under this heading include gear mesh arrangement, torsional spring, and fisher wire.

Two gears are utilized in the mechanism for the gear mesh arrangements. One governs the speed of the motor deploying the arms, employing a fisher wire to secure the arms against the spring, while the second gear facilitates solar tracking and can adjust up to a 45-degree angle on either side of the yoke. *Fig. 7* and *Fig. 8* depict the pictorial and orthographic views of the tilt gears, including their attachment points to the servo motor.

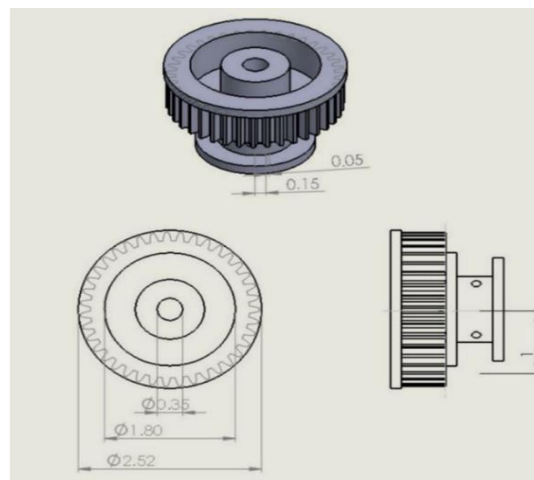
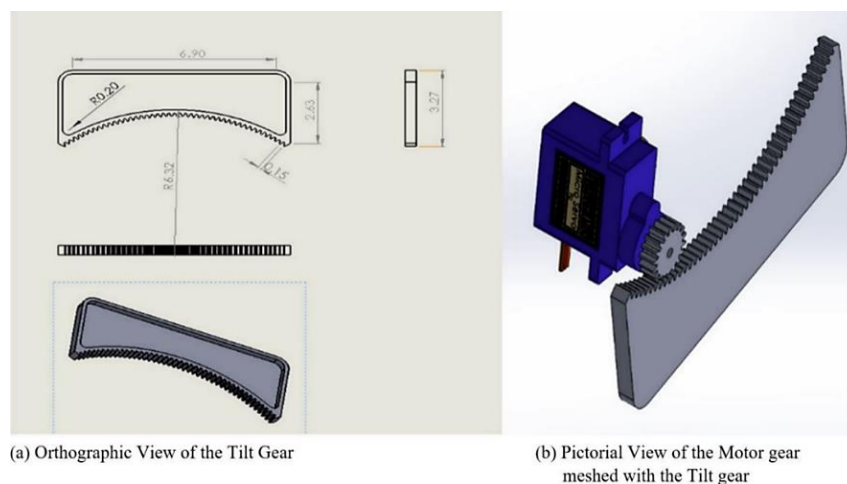


Fig. 7. Orthographic view of the arm gear.



(a) Orthographic View of the Tilt Gear

(b) Pictorial View of the Motor gear meshed with the Tilt gear

Fig. 8. Diagram of the tilt Gear.

The torsion spring, illustrated in *Fig. 9*, is designed to gradually deploy the solar panels to a 90-degree angle. The initial stage of designing the torsion spring involved calculating essential parameters based on the fundamental principles of Hooke's Law.

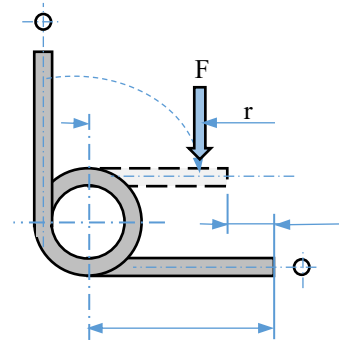


Fig. 9. a. Torsional spring for deployment initiation.

Springs obey the angular form of Hooke's Law, which states that the force needed to extend or compress a spring is proportional to the change in the length of the spring". In further buttressing this basic assumption, the following computations were made.

The fisher wire is a nylon string that holds the deploying panels against the deployment springs so that, at any instance, the arms cannot move freely due to their momentum to prevent oscillation when momentum is reversed. It has a density of 1140 kg/m<sup>3</sup> and a 40–100 MPa strength.

### 2.3.3 | The drive system

This comprises two servo motors – an arm motor and a tilt motor connected to a gear train for deployment and solar tracking, respectively, and a circuit board for system control. The arm motor is attached with a 3 mm screw to the arm holder and is linked to the two wings with a fishing wire, while the tilt motor rotates the arm assembly through 45° on each side for solar tracking. Servo motors SG-90 model with an operating voltage of ~5V, a torque of 1.8 kgf-cm, and an operating speed of 100 rpm.

## 2.4 | Analyses of the System Operating Parameters

### 2.4.1 | Torque exerted on the panels

The torque exerted by the panels is given by load times the distance from the center of gravity of the planes to the hinge (i.e., ½ of the panel length. Refer to Fig. 9.b).

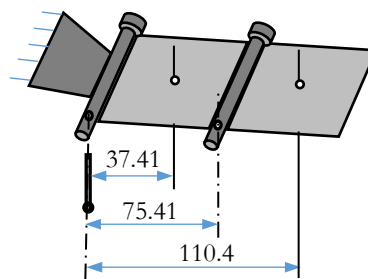


Fig. 9. b. Mass centers of the components of the solar panel assembly

The total length of panels,  $L_1 = L_2 = 70$  mm and the width  $W = 110$  mm.

Mass per =  $0.07 * 0.11 * 0.25 = 1.925$  g/solar sheet.

Mass of top panel (thickness 1.5 mm) =  $0.07 * 0.11 * 0.0015 * 1050 = 12.1275$  g.

Mass of the printed panel arms:  $M_1 = 6.1520$  g and  $M_2 = 12.1268$  g.

Mass of the hinge pins ( $d = 3$  mm and  $lw = 117.5$  mm and density of T-304 = 7930 kg/m<sup>3</sup>),

$$M_p = \pi * \frac{0.003^2}{4} * 0.1175 * 7930 = 6.586. \text{ g.}$$

Mass of spring (ASTM 313, density = 79165 kg/m<sup>3</sup>,  $d = 1.5$  mm,  $D_m = 5$  mm, 8.75 turns),



$$M_s = \pi * \frac{0.002^2}{4} * \left[ \pi * \frac{(5-1.5)}{1000} * 8.75 \right] * 7930 = 2.3969 \text{ g.}$$

Mass of fisher wire (density = 939 kg/m<sup>3</sup>, d = 2 mm, D<sub>m</sub> = 5 mm, and l = 1.25 (145.41 + 2 πD)),

$$M_f = \pi * \frac{0.002^2}{4} * \left( 1.25 * \frac{(145.41+2*5.15)}{1000} \right) * 1140 = 0.6971 \text{ g.}$$

Total weight of arm 1, M<sub>t1</sub> = (Mass of Solar cells + Mass of the Panels + Mass of the arms) \* 9.81 = (1.9250 + 12.1275 + 6.1520)/1000 \* 9.81 = 0.1982 N.

Total weight of arm 2, M<sub>t2</sub> = Mass of Solar cells + Mass of the Panels + Mass of the arms + mass of pin = (1.9250 + 12.1275 + 12.1268)/1000 \* 9.81 = 0.2568 N.

Thus, the torque, τ = (0.1982 \* 0.03741) + (0.2568 \* 0.11041) +  $\left( \frac{6.586*0.07541}{1000} + * \frac{0.6971}{1000} * \frac{0.1946}{2} \right) * 9.81 = 0.0413 \text{ Nm.}$

### 2.4.2 | Torque constant or spring stiffness

The torsion constant or spring stiffness is the value that determines how much torque is required to move the spring through a given angle, as given in *Eq. (1)*.

$$\tau = k\theta \rightarrow k = \tau/\theta, \tag{1}$$

where, τ = applied torque (or designed torque), k = spring Stiffness and θ = angular displacement.

F/τ = force / torque.

k = spring stiffness.

x/θ = distance / displacement angle = 90° or 1.571 rad k = 0.0247/1.571.

k = 0.016 Nm/rad.

### 2.4.3 | Angular velocity

The maximum angular velocity of the panel can be obtained using conservation of potential energy, Pe stored in the spring while being twisted, and Ke released when it is unwounded as given in *Eqs. (2)-(4)*:

$$\text{The potential energy stored in the spring } P_e = 1/2k(\theta_2^2 - \theta_1^2). \tag{2}$$

$$\text{Kinetic Energy } K_e = 1/2I * \omega^2. \tag{3}$$

$$\omega = \sqrt{\frac{2K.E}{I}}, \tag{4}$$

Where Pe = the potential energy, Ke = the kinetic energy, I = the moment of inertia, θ = angular displacement, K = the spring constant, and ω = the angular velocity.

The torsion spring is compressed when in a stowed position (when the panels are folded). At this point, when no work is done on the mass (panels arms), the potential energy stored in the spring is the same as the initial kinetic energy by energy conservation at the instance of the spring release. Thus, the maximum velocity is given in *Eq. (5)* as Ke = Pe:

$$\omega = \sqrt{\frac{2P_e}{I}}. \tag{5}$$

Therefore, setting P.E = K.E yields *Eq. (5)* and substituting the appropriate parameter values gives.

$$\omega = \sqrt{\frac{2 \times 0.019}{9.5 \times 10^{-5}}}$$

$$\omega = 20.260 \text{ rad/sec.}$$

### 2.4.4 | Angular acceleration

From equations of motion, the torque exerted by the spring on the panel is equal to the moment of inertia times the angular acceleration as given in Eq. (6).

$$\tau = I \times \alpha. \quad (6)$$

$$\text{But } I = \frac{1}{12} M(L^2 + W^2). \quad (7)$$

$L = 140 \text{ mm}$ ,  $W = 110 \text{ mm}$ ,  $M = 0.036 \text{ kg}$ .

$$\text{From Eq. (6), actual angular acceleration } \alpha = \frac{\tau}{I} = \frac{0.0413}{9.5 \times 10^{-5}}.$$

$$\alpha = \frac{\tau}{I}.$$

$\alpha = 435 \text{ rad/sec}^2$  per arm with 100% shock safety margin.

### 2.4.5 | Deployment time

Time for complete deployment of the panel with respect to the angular displacement  $90^\circ$  was obtained from the basic angular velocity equation.

$$\alpha = \frac{\Delta\omega}{\Delta t} \rightarrow \omega = \frac{\Delta\theta}{\Delta t}, \quad (8)$$

Where  $\omega$  = angular velocity,  $\theta$  = angular displacement,  $t$  = time, and  $\frac{\Delta\theta}{\Delta t}$  = the rate of angular displacement.

Between two close-time instances, the average time required for complete deployment is given as:

$$\Delta t = \frac{\Delta\theta}{\omega}. \quad (9)$$

For  $\omega = 20.260 \frac{\text{rad}}{\text{s}}$ , and  $\theta = \frac{\pi}{2} \text{ rad}$ , the time required for complete deployment is.

$$t = 0.077 \text{ s}.$$

This time is, however, too short and could result in panel oscillation due to reverse momentum as it flies to hit the backrest within a short time. The time was relaxed to 2 seconds using fisher wire string to constantly hold the panels against the spring, thus taking them to the rest positions with minimum disturbance.

## 2.5 | Selection of the Deployment Drivers and Actuators

### 2.5.1 | Motor sizing

Three major factors were considered when sizing the motor: load inertia, motor torque (i.e., torque from external forces), and operating speed.

Load Inertia: from Eq. (7), the load inertia  $I = 9.5 \times 10^{-5} \text{ kgm}^2$ .

Torque of the motor: the torque,  $T$ , required = Total countering forces \* ratio of arm length.

The motor is to drive the two arms of the wings. Thus, the Total countering torque is:

$$T_t = \text{Torque on arm 1 component } T_1 + \text{Torque on arm 2 component } T_2.$$

For the two arms,  $T_t = 0.0413 \times 2 = 0.0826 \text{ Nm}$ .

For a shock torque factor of 100%,  $T = 0.1652 \text{ Nm}$ .

Or, from Fig. 5, the ratio of the arm to yoke =  $145.41/35.64 \approx 4$ .

Using a shock factor of 4, the torque required by the motor is  $0.0413 \times 4 = 0.1652 \text{ Nm}$ .



Hence, an SG-90 servo motor was selected with a torque of 0.1765 Nm (1.8 kgcm)

Motor operating speed and time:

$$N = 60\omega/p_d G, \quad (10)$$

where,

$N$  = rotating speed of a motor in rpm.

$\omega$  = angular velocity in rad/s.

$p_d$  = ball screw pitch in mm.

$G$  = gear ratio.

$$\omega = \frac{\Delta\theta}{\Delta t} = \frac{90}{2} = 45^\circ/s = 7.5 \text{ rpm.}$$

Assuming deployment time  $t = 2$  secs.

Gear ratio  $G = \text{driven gear } g_1 / \text{motor gear } g_2$ .

$$G = 39/14 = 2.785.$$

$$N = \frac{60 * 7.5}{3.5 * 2.73} = 47.1 \text{ rpm.}$$

$$\text{Power, } P = TN, \quad (11)$$

where,

$P$  = power W.

$T$  = torque Nm.

$N$  = speed of motor rpm.

$$P = 0.1765 * 47.1.$$

$$P = 8.3 \text{ W.}$$

$$\text{But the electric power is given as } P = IV, \quad (12)$$

where,

$P$  = power W.

$I$  = current A.

$v$  = voltage V.

A voltage of 5V was chosen since the power rating is low and falls within the standard values.

$$I = P/V \rightarrow \text{Therefore, } I = 18/5 = 3.72 \text{ A.}$$

The final design motor parameters are:

$$\text{Current } I = 3.72 \text{ A, Voltage } V = 5\text{V, Speed} = 47.1 \text{ rpm, Torque} = 0.1765 \text{ Nm.}$$

The spring initially imparts angular velocity to the panels upon release, starting at  $\theta = 90^\circ$  and decreasing gradually to zero at  $\theta = 0^\circ$ . The chosen release spring configuration features two arms extended at right angles to each other. While one arm is fixed against a frame, the other is depressible. This configuration is depicted in *Fig. 9*.

$$S = \frac{32M}{\pi d^3} K_b \rightarrow d = \sqrt[3]{\frac{32\tau}{\pi S} K_b}. \quad (13)$$

$$\text{Where the stress correction faction: } K_b = \frac{4C^2 - C - 1}{4C(C-1)}. \quad (14)$$

and,

$d$  = wire diameter.

$M$  = moment or torque.

$\tau$  = moment or torque.

$S$  = maximum design stress.

For spring index  $C = 6$ ,  $K_b = 1.1417$ . For a wing, the maximum torque load is 0.0413 Nm. Stainless steel material was considered based on ASTM A313 standard, and the yield stress of stainless steel is  $S_y = 585$  MPa. As stated in the literature [2], for Standard 302, the maximum design stress  $S$  for stainless steel equals 60 to 70% of the minimum yield strength of the material. Using a minimum requirement,

$S = 60\%$  of 585 MPa = 409.5 MPa.

Thus, the wire diameter is  $d = \sqrt[3]{\frac{32 * 0.0413}{\pi * 409.5 * 10^6} * 1.1417} = 1.05$  mm.

The material's modulus of elasticity is considered, and the spring wire diameter is obtained based on geometry.

$$D = \left[ \frac{64\tau D_m}{E\theta} * \left( N_b + \frac{l_1 + l_2}{3\pi D_m} \right) \right]^{1/4}, \quad (15)$$

Where,

$\tau$  = applied torque.

$D_m$  = coil mean diameter.

$E$  = the modulus of elasticity.

$N_b$  = number of body coils (active coils + twisted coils).

$l_1$  = length of free leg.

$l_2$  = length of twisted leg.

A clearance of 10% over the hinge pin was adopted to avoid excessive friction at the spring-pin interface. Thus, for the hinge pin diameter of 3 mm used, the minimum internal diameter of the required spring is 3.3 mm. When installed position, the spring legs are entirely displaced through 90°, under the influence of the applied torque  $\tau$ . The stainless steel material has a yield stress of 585 MPa based on ASTM A313 standard. The active coils are taken to be 8.5 with a twist coil fraction of 0.25 over 90°. The free leg is 16 mm, and the twisted one is 12.07 mm. The required spring wire diameter is:

$$d = \left[ \frac{64 * 0.0413 * 0.005}{585 * 10^6 * 0.6 * 90} * \left( (8.5 + 0.25) + \frac{0.016 + 0.01207}{3 * \pi * 0.005} \right) \right]^{1/4} = 0.0014062 \text{ m.}$$

The stress indicated a spring wire of 1.05 mm is adequate, while from geometry, 1.41 mm is adequate. Since geometry is higher than the stress-dependent value, a 1.5 mm spring wire was selected.

### 2.5.2 | Fisher wire diameter

From section 2.4.1, the torque exerted by the springs on the panels is a function of the panel weight and the spring arm length. The panel weight is made of the following components: the mass of the solar cells, the

mass of the panels, the mass of the arms that hold them together, the mass of the hinge joint pin, the mass of the springs, and the mass of the fisher wire. Thus, the total load is calculated from:

$$W_T = (2m_s + 2m_p + m_{a1} + m_{a2} + m_p + m_s + m_f) * g, \quad (16)$$

where  $m_s$  is the mass of Solar cells,  $m_p$  is the mass of the Panels,  $m_a$  is the mass of the arms,  $g$  is the acceleration due to gravity. Thus, from Eq. (16), the total load supported by the string is:

$$W_t = (2*1.925+2*12.128+6.152+12.127+6.586+2.958+0.697)/1000*9.81 = 0.5555 \text{ N.}$$

The tension spring was modeled to dampen the vibration excitation from the torque exerted by the spring. With the assumption that both the strings will, thus, vibrate with the same frequency as the panels, the frequency of the wire is given by Lynch and Jim [3] as:

$$f = \frac{1}{2l} * \sqrt{\frac{T}{\mu}}, \quad (17)$$

Where,

$f$  = the first fundamental frequency.

$T$  = tension in the string, which is taken to be equal to the weight of the panel assembly.

$l$  = length of the string.

$\mu$  = the mass per unit length of the string used ( $=0.6476d^2/\text{meter}$ ).

The length of the fisher wire is taken to be:

$$l = 1.25 (145.41 + 2 \pi d_p) = 1.25 * (145.41 + 2 * \pi * 0.003) = 181.786 \text{ mm.}$$

$$T = W_T = 0.5555 \text{ N.}$$

$$\text{Thus, } f = \frac{1}{2*0.181786} * \sqrt{\frac{0.5555}{0.6476*d^2}}.$$

The associated stress in the string due to the tension, as expressed by Oldrich [4], is:

$$\sigma = \frac{16 * f^2 * L^2 * \mu}{\pi * d^2}, \quad (18)$$

Where,

$\sigma$  = the stress in the string under the applied load.

$d$  = is the required string diameter.

So that:

$$\sigma = \frac{16 * \left( \frac{1}{2 * 0.181786} * \sqrt{\frac{0.5555}{0.6476 * d^2}} \right)^2 * 0.181786^2 * 0.6476 * d^2}{\pi * d^2}.$$

For a tensile strength of 40 MPa and a fatigue performance criteria 3a, a factor of safety of 10, the diameter from 0.0004205 m. This is relatively too small for handling and will exert enormous pressure on the point of contact during vibration; thus, a further factor of 3 due to forced frequency is used. This brings the diameter to 1.26 mm.

From Eq. (18), the required diameter  $d$  for the stiff string to hold the panels firmly against the spring is determined. The tensile strength of the material for the string is used as the basis, while the length of the string is determined from the sum of the panel lengths, the circumferences of the pulleys used, and 25% of the total length to anchor the string to panel-2 and the driving motor-shaft.

The selection of fisher thread is characterized by its twine numeration, which is indicated by numbers,  $N_g$  (length per gram of the thread), and the number of strands,  $n$ , composing the thread. It is commercially quoted as a fraction,  $N_g/n$ , and referred to as the structural number of the thread. In selecting the thread, the length  $l$  is first measured in meters, and the weight measured in grams. The manufacturers quote the number of strands,  $n$ . A multi-twine thread is used to improve strength against fatigue. The number of twines,  $N_t$  required is obtained from the relation Baranov [5]:

$$N_t = u * n * \left(\frac{1}{\mu}\right), \quad (19)$$

where  $u$  is the correction coefficient for the degree of shortness for twined threads ( $u = 1.05$  for nylon [3]), the number,  $n$ , is commercially quoted for the number of strands, and  $m$  is the weight of the string in grams.

For  $u = 1.05$ ,  $n = 9$  (in 3x3) and  $\mu = 0.6476 * d^2 = 0.6476 * (0.002)^2 = 2.5904 \text{ g/m}$ .

Thus  $N_t = 1.05 * 9 * 2.5904 = 24.48$ .

From the  $N_t$ - $dt$  commercial collections shown in *Table 1*, the right diameter falls between 1.85 and 1.98 mm, which is adequate. A 2.0 mm thread was chosen.

**Table 1. Thread diameter versus commercial ID number.**

Commercial number, $N_t$	18	21	24	30	36	48	60	72
Thread diameter, $dt$ (mm)	1.52	1.70	1.85	1.98	2.16	2.55	2.95	3.17

The diameter selected must be greater than the value obtained from the thread analysis. Thus, 2 mm was chosen as an adequate size.

### 2.5.3 | Projected area of panels for solar rays

The energy generated in a solar panel depends largely on the surface area available to receive solar energy from the sun. With a panel of length  $L$  and width  $W$ , the maximum available area for solar panels will be  $L * W$ . However, this assumes the plane of the panels will be at a right angle to the sun's rays. This is not always possible in the case of solar panel arms in CubeSat due to two main angular displacements associated with their deployments and operations.

- I. Unfolding of the panels: the panels are normally folded and stowed on the opposite sides of the CubeSat's frame until it is deployed. During deployment, the folded panels gradually open up from  $0^\circ$  inclination angle up to about  $90^\circ$  when it is fully opened, during this period, the surface of the panel area will not be fully available for the sun's exposure. This is also the case when the panel swings or oscillates during eclipsing.
- II. Secondly, as the CubeSat floats, it continually changes the panel surface areas away from the sun's rays. With a tracking system in place, the photo-electric cell is being revved back to the sun's rays. Also, during this phase, the panels are not directly facing the sun. When the rays are parallel to the plane of the panels, their reception is assumed to be minimal and gets maximal when directly facing it at  $90^\circ$ .

In these conditions discussed, the energy generated depends on solar availability and the projected area of panels for the reception of the sun's rays.

Projected area refers to the percentage equivalent area at any angular position of the panels that will provide the same quantity of energy when the panel is at  $90^\circ$ . With this definition, the power generated is obtained from Ehren [45]:

$$E = \eta * SI * [A * \cos(\varphi) * \sin(\theta)]. \quad (20)$$

where  $\eta$  is the solar cell efficiency given as 20.4% from the manufacturer,  $SI$  is the solar intensity constant whose value is taken to be  $1361 \text{ W/m}^2$ , is the area of the panels obtained from  $L * W * \alpha_p$  and the angular

displacements  $\varphi$  and  $\theta$  represent the incident ray angles, respectively, the tilt angle of tracking and half of the inclination angle between the panels during unfolding or vibration. Panel area availability factor,  $\alpha_p = 0.92$ .

### 3 | Results

#### 3.1 | The Synthesized Design of the Deployment Mechanism and Components

The key components synthesized in the design of the SADM are shown in *Fig. 10*.

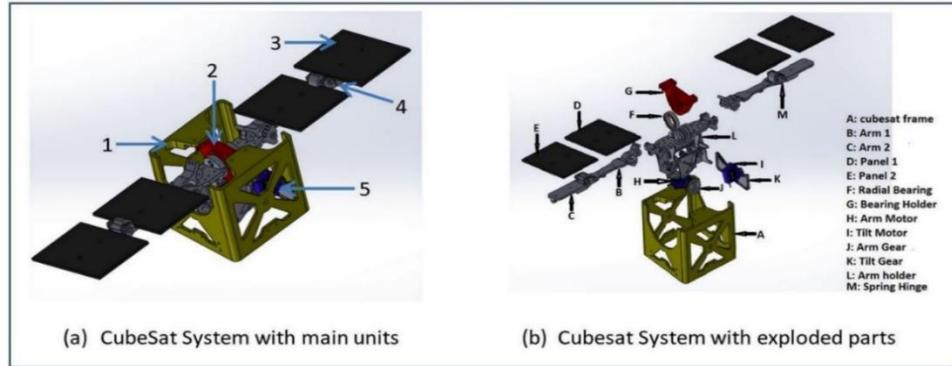


**Fig. 10.** Assemble model of the designed solar array deployment mechanism.

In the same vein, a pictorial view of the 3D print of the model is shown in *Fig. 11*, with the main parts labeled.

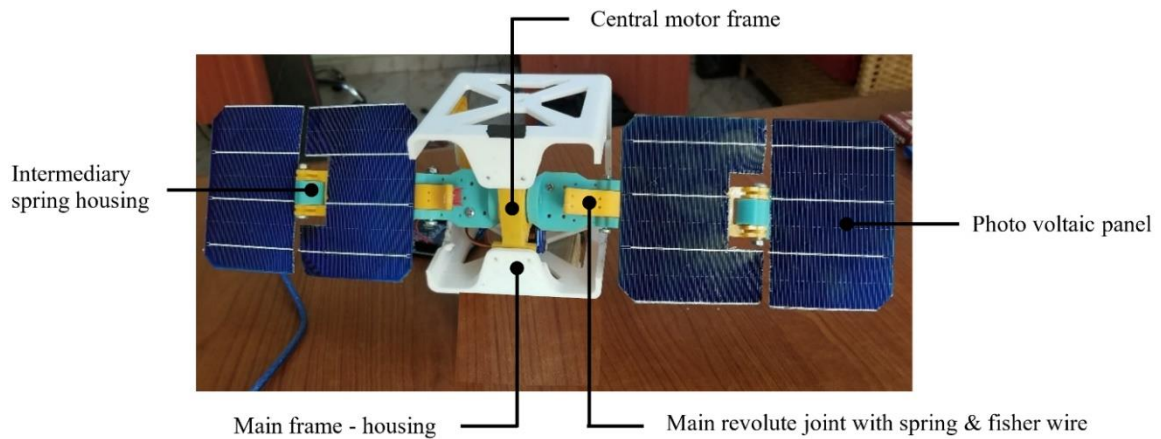


**Fig. 11.** Developed and assembled deployable solar arrays.

#### 3.2 | Design Dimensions and Operating Parameters

*Table 2* provides the final dimensions and operational parameters for the components involved in the solar array deployment.

**Table 2.** Panel and release spring design parameters.

Design Parameter	Value	Unit
Length of panels, $L_p$	0.07	(m)
Width of panels, $w_p$	0.11	(m)
The thickness of the panel $t_p$	0.003	(m)
Mass of panels $m_p$	0.018	(kg)
Spring max, Deflection, $\theta_{max}$	1.571	(rad)
Torque on panels, $\tau_1$	0.0247	(Nm)
Spring constant, $K$	0.0157	(Nm/rad)
Total deployment time, $t$	0.0777	(sec)
Initial angular velocity, $\omega$	20.2084	(rad/sec)

## 4 | Discussion

### 4.1 | The Synthesized Design of the Deployment Mechanism and Components

The key components of the deployable solar array system depicted in *Fig. 10(a)* include the main body (CubeSat sidewall) labeled as 1, yokes labeled as 2, panel frames labeled as 3, torsion spring and hinge labeled as 4, and DC servo motor labeled as 5.

The main body serves as the nucleus point, housing and anchoring all components. A pivotal yoke mounted on the main body secures the panel arms and facilitates the rotation of a series of foldable solar array arms. Each array comprises two symmetrical wings, with two arms hinged together and connected to the arm holder via torsion spring hinges to transition the panel array from stowed to deployed positions.

Each arm is affixed to a servo motor shaft via a bearing, which allows the yoke to rotate up to 90 degrees, tracking the sun's rays. A DC servo motor acts as the primary actuator for driving these movable parts. Other integral components include a DC battery for storing and supplying power required for system operations and a system circuit board for managing connections, signals, and controls. These components are not detailed further in this manuscript, as previously explained in the opening paragraph of Section 2.3.

The solar panel wings are stowed in a folded configuration against the CubeSat's side walls, held in place by an HDRM. Upon command from the remote control, the hold-down pin is disengaged, allowing the tensioned spring to unwind and deploy the wings into a horizontal position.

Kinematic analysis was conducted on the CubeSat's solar panel arrays featuring a passive deployment mechanism and integrated tension fisher-wire for speed control during deployment. This system was modeled, simulated, and fabricated to adhere to the recommended weight and spatial dimensions outlined in the literature [6].

We decided to use lighter strings for future implementation to reduce weight and spatial requirements compared to traditional electro-mechanical deployment mechanisms. However, the absence of holdback locks, which prevent panels from rebounding and compressing the torsion spring, could reduce power generation and fatigue at the hinges, as highlighted by Arturo et al. [7].

This article proposes modifications focused on optimizing component sizing and kinematic parameters to enhance space and weight efficiency, ensure system stability during panel array deployment and operation, and optimize photovoltaic surface orientation for maximum power generation from solar rays.

### 4.2 | Design Dimensions and Operating Parameters

*Table 1* provides the final dimensions and operational parameters for the components involved in the solar array deployment. This includes the spring and panel design parameters based on the geometric specifications and design of a 1-U CubeSat derived from *Eqs. (1)-(19)*.

Highlighted in *Table 1* are the key parameters of the spring design. The spring needs an overall stiffness of 0.0157 Nm/rad to move the solar panels with a resultant torque of 0.0247 Nm from 0° to 90°. The entire panel deployment occurs in just 0.0777 seconds, with an angular velocity of 20.2084 rad/sec. Due to the very short deployment time (0.0777 sec), the velocity is high, resulting in significant momentum.

Based on the standard size reported by Theoharis et al. [6], the current model is a 1U CubeSat with geometric dimensions of 105 mm x 103 mm x 107 mm (in launch configuration). The model features two opposite wings, each with two panel mounts, each 70 mm long. The inter-panel hinge space is 5.41 mm to allow for free rotation, and the yoke length is 35.64 mm, resulting in a combined wingspan of 181.05 mm. With a limiting width of about 100 mm, the maximum combined (end-to-end) length for two foldable mounts (arms) was set not to exceed 200 mm on each side of the CubeSat. This requirement is met as the model's end-to-end arm length is 181.05 mm, 90.5% of the standard maximum cross-sectional dimension.



A similar model, the NEE-01 PEGASUS launched by the Ecuadorian Civilian Space Agency (ECSA) in 2013 [7], has dimensions of 100 mm x 100 mm x 100 mm (in launch configuration) and a mass of approximately 1.26 kg. It features two solar panel wings, each with three panels for a total of six panels per wing. The deployed dimensions are 100 mm x 100 mm x 750 mm with a panel thickness of 1.5 mm.

The weight of the 3-D printed housing frame, with a thickness of approximately 3.5 mm and about 37.9% void area, is 110.4 g. Two servo motors weigh 36 g each, a gear train assembly weighs 27.8 g for the speed control line, and a solar tracking gear train weighs 43.5 g. The arms and yoke, printed from high-performance PLA thermoplastic material with a 1240 kg/m<sup>3</sup> density, weigh 139.3 g. The panels, made from compressed paper bonded with resin adhesive with a 1201 kg/m<sup>3</sup> density, weigh 188.58 g. The overall weight of the CubeSat with the two opposite wings is 0.8375 kg from simulation and 0.942 kg from physical measurement. The difference, about 11%, is due to plastic welding materials, joining links, and inaccuracies in measuring hard-to-reach void areas. However, both values are within the standard weight for a CubeSat, with the physical measurement leaving about 29% of its standard weight for communication systems. This indicates that the CubeSat will meet the maximum space and weight criteria for proper operation.

The solar array assembly accounts for about 49.2% of the CubeSat's weight. Imbalance during operation can result in low power output and fatigue at the hinges, as reported in [1]. As the panels reach their final positions, they hit the hinges and rebound with a relatively higher velocity. Although these rebounds generate vibrations within the system, introducing fisher wire creates damping effects. The dynamics of the generated vibration and control were discussed in another article.

The total area available is  $110 \times 70 \times 4 = 0.0308 \text{ m}^2$  with availability of about 70%.

## 5 | Conclusion

The work focused on developing a SADM for a 1-U CubeSat using locally sourced materials. The design calculations and generated parameters guided the construction of the project's parts (with a few material substitutions). Due to the unavailability of the locally designed torsion spring, it was replaced with an elastic band of the same texture. The project was successfully tested, showing minimal variance and adjustments from the calculated parameters and design materials. The elastic band tension holds the solar panels in a stowed (vertical) position, and they deploy in approximately 2 seconds with a speed of 47.1 rpm. Additionally, the panels' tilt capability towards the sun generates enough energy to sustain the CubeSat, outperforming fixed or body-mounted configurations.

## List of Abbreviations

Not applicable.

## Declarations

Ethics approval and consent to participate do not apply to this research.

Consent for publication: this does not apply to this manuscript.

Availability of data and material: this does not apply to this manuscript.

Competing interests: there are no competing interests to declare concerning the content of this manuscript.

## Funding

The research reported in this manuscript was self-sponsored.

## Authors contribution

IBU generated the theories and undertook the draft of the article, while NML carried out the SolidWorks modeling and analysis, as well as read through and contributed to the writing of the final manuscript. All authors have read and approved the manuscript.

## Acknowledgments

The authors wish to thank Ms Dorin Nwachukwu for her contributions to 3D printing and other peripheral works.

## References

- [1] Solís-Santomé, A., Urriolagoitia-Sosa, G., Romero-Ángeles, B., Torres-San Miguel, C. R., Hernández-Gómez, J. J., Medina-Sánchez, I., ... & Urriolagoitia-Calderon, G. (2019). Conceptual design and finite element method validation of a new type of self-locking hinge for deployable CubeSat solar panels. *Advances in mechanical engineering*, 11(1). DOI: 10.1177/1687814018823116
- [2] Nisbett, K., & Budynas, R. (2015). *Shigley's mechanical engineering design (10th ed.)*. Y McGraw-Hill Education, 2 Penn Plaza, New York.  
[https://www.researchgate.net/publication/323744834\\_Shigley's\\_Mechanical\\_Engineering\\_Design\\_10th\\_Edition](https://www.researchgate.net/publication/323744834_Shigley's_Mechanical_Engineering_Design_10th_Edition)
- [3] Lynch-Aird, N. (2017). Mechanical properties of nylon harp strings. *MDPI*, 10(5), 497. DOI: 10.3390/ma10050497
- [4] Dajbych, O. (2019). Ultimate tensile strength of the string determination using spectral analysis. *7th tae*, 113–116. <https://2019.tae-conference.cz/proceeding/TAE2019-020-Oldrich-Dajbych.pdf>
- [5] Baranov, F. I. (1948). *Theory and estimation of fishing gear*. Fish industry press.  
<http://www.nativefishlab.net/library/textpdf/15559.pdf>
- [6] Liu, S., Theoharis, P., Raad, R., Tubbal, F., Theoharis, A., Iranmanesh, S., ... Matekovits, L. (2022). A survey on CubeSat missions and their antenna designs. *Electronics*, 11(13), 1–46. DOI: 10.3390/electronics11132021
- [7] Solís-Santomé, A., Urriolagoitia-Sosa, G., Romero-Ángeles, B., Torres-San Miguel, C. R., Hernández-Gómez, J. J., Medina-Sánchez, I., ... Urriolagoitia-Calderon, G. (2019). Conceptual design and finite element method validation of a new type of self-locking hinge for deployable CubeSat solar panels. *Advances in mechanical engineering*, 11(1). DOI: 10.1177/1687814018823116